MDPI

*Article*

# Dielectric Properties of $Mg_2TiO_4$-Doped $Ca_{0.65}Sr_{0.35}Zr_{0.65}Ti_{0.35}O_3$ with High Withstand Voltage and Low Loss

**Yun Liu, Binbin Huang, Xiaoyang Chen and Ping Yu ***

College of Material Science and Engineering, Sichuan University, Chengdu 610064, China; liuyun6@stu.scu.edu.cn (Y.L.); huangbinbin@stu.scu.edu.cn (B.H.); xiaoyang189@scu.edu.cn (X.C.)
* Correspondence: pingyu@scu.edu.cn

**Abstract:** $Mg_2TiO_4$-doped $Ca_{0.65}Sr_{0.35}Zr_{0.65}Ti_{0.35}O_3$ (CSZT) thin films with different $Mg_2TiO_4$ concentrations were deposited on the $LaNiO_3$(LNO)/p-Si substrate using radio-frequency magnetron sputtering technology. The dielectric response of the prepared x% $Mg_2TiO_4$-CSZT thin films with frequency, voltage, and temperature was systematically studied. The tanδ and leakage current density of CSZT thin films were reduced effectively by introducing $Mg_2TiO_4$ content. The prepared 6% $Mg_2TiO_4$-CSZT thin film, due to its low loss (tanδ ~0.01 at 1 MHz), satisfied temperature stability (TCC ~−68 ppm/°C, from −55 °C to 205 °C), high withstand voltage (>160 V), and small leakage current density (about $3.34 \times 10^{-6}$ A/cm$^2$ at operating voltage of 160 V). This may be useful for capacitor materials in the next generation of portable electronic systems.

**Keywords:** linear dielectric thin films; RF magnetron sputtering

**Citation:** Liu, Y.; Huang, B.; Chen, X.; Yu, P. Dielectric Properties of $Mg_2TiO_4$-Doped $Ca_{0.65}Sr_{0.35}Zr_{0.65}Ti_{0.35}O_3$ with High Withstand Voltage and Low Loss. *Crystals* **2022**, *12*, 405. https://doi.org/10.3390/cryst12030405

Academic Editor: Shujun Zhang

Received: 9 February 2022
Accepted: 15 March 2022
Published: 16 March 2022

**Publisher's Note:** MDPI stays neutral with regard to jurisdictional claims in published maps and institutional affiliations.

**Copyright:** © 2022 by the authors. Licensee MDPI, Basel, Switzerland. This article is an open access article distributed under the terms and conditions of the Creative Commons Attribution (CC BY) license (https://creativecommons.org/licenses/by/4.0/).

## 1. Introduction

Thin film capacitors are considered one of the most strategic technologies for future integral capacitors to meet the needs of miniaturized electronic equipment [1–4]. Among them, the thin film chip capacitors are recommended as candidate products in the field of handheld products. It is agreed that the dielectrics with satisfied stability in frequency, voltage, and temperature are still the key capacitor materials in the next generation portable electronic systems. Linear dielectric thin films are expected to be candidate materials for the next generation of integrated capacitor materials due to their high dielectric breakdown strength, low loss, and high stability in frequency and temperature [5]. However, traditional linear dielectrics such as $SiO_2$, $Al_2O_3$, and $Ta_2O_5$, etc., are limited to achieve a high specific capacitance due to their low dielectric constant [6–8] (ε ~3.9 for $SiO_2$, ~7 for $Al_2O_3$, ~26 for $Ta_2O_5$).

For decades, different approaches have been carried out to develop high dielectric response performance dielectric thin films. It is notable that the high dielectric permittivity of 55 was achieved in $(Ca_{0.7}Sr_{0.3})(Zr_{0.8}Ti_{0.2})O_3$ thin films by Lee et al. [9]. The loss of $(Ca_{0.7}Sr_{0.3})(Zr_{0.8}Ti_{0.2})O_3$ thin films was 0.015 at 1 MHz, and the leakage current density reach to $5 \times 10^{-6}$ A/cm$^2$ at voltage of 12 V [10]. The results show that the $(Ca_{0.7}Sr_{0.3})(Zr_{0.8}Ti_{0.2})O_3$ thin film could be one of the most potential materials in the field of advanced capacitors. Similar research was reported in the $Ca_{0.65}Sr_{0.35}Zr_{0.65}Ti_{0.35}O_3$(CSZT) thin films on Pt/$SiO_2$/Si substrate by our group [11]. At room temperature, the dielectric permittivity, $\varepsilon_r$ ~56.4, low tanδ ~0.003 at 1 MHz and leakage current density ~$1.1 \times 10^{-7}$ A/cm$^2$ at the bias voltage of 80 V were achieved. Further investigations reveal that the loss of the CSZT thin films on p-type Si substrate is higher than that on Pt/$SiO_2$/Si substrate and the TCC (temperature coefficient of capacitance) increased from +23.3 ppm/°C to +135 ppm/°C. For a practical integral capacitor application, p-type Si substrate is a more flexible choice. The development and improvement of the dielectric properties of CSZT thin films deposited on p-type Si substrate are necessary.

$LaNiO_3$ (LNO) is a type of metallic oxide with a pseudo-cubic structure and is often used as a buffer layer to eliminate the interfacial dead layer between the ferroelectric thin

film and the Pt electrode [12–14]. In addition, LNO was reported with the capability of contributing to the preferential orientation growth in lots of $ABO_3$ thin films [15,16]. Preferential orientation has been proven as an important approach to enhance the performance of the thin films. Therefore, the LNO layer was also used in this work as a buffer layer between the CSZT and p-type silicon substrate.

In present work, the dielectric properties of $Mg_2TiO_4$-doped CSZT thin films are reported. Previous studies have reported that non-ferroelectric materials, such as MgO, $MgTiO_3$, $Mg_2TiO_4$, $Mg_2SiO_4$, $BaTi_4O_9$, etc., are helpful to reduce the dielectric loss [17–24]. The x% $Mg_2TiO_4$-CSZT thin films were deposited on LNO/p-Si by radio frequency magnetron sputtering technology and the LNO was deposited as buffer between the CSZT thin film and the p-type silicon substrate. The work aimed to obtain a reliable high performance thin film for capacitor application which not only has a moderate dielectric permittivity and low loss, but also small TCC in wide temperature range.

## 2. Experiments

In this work, sol-gel process was employed to synthesis x% $Mg_2TiO_4$ doped CSZT and LNO powders, respectively. The targets used to prepare x% $Mg_2TiO_4$ doped CSZT thin film and LNO buffer layer were made of the x% $Mg_2TiO_4$ doped CSZT and LNO powders, respectively. The $Ca(CH_3COOH)_2{\cdot}2H_2O$ (Aladdin, 98%), $Sr(NO_3)_2$ (Chron, 99.5%), $Ti(OC_4H_9)_4$ (Aladdin, 98.5%), $Zr(NO_3)_4{\cdot}5H_2O$ (Chron, 99.28%), and $Mg(CH_3COO)_2{\cdot}4H_2O$ (Greagent, 99.0%), weighted according to the x mol% $Mg_2TiO_4$ - $Ca_{0.65}Sr_{0.35}Zr_{0.65}Ti_{0.35}O_3$ stoichiometry, were used to synthesize x% $Mg_2TiO_4$ doped CSZT precursor sols. The $LaNiO_3$ stoichiometric $La(NO_3)_3{\cdot}$ $6H_2O$ (Chron, 99.00%) and $Ni(CH_3COO)_2 \cdot 4H_2O$ (Chron, 98.00%) were weighted to synthesize LNO precursor sol. After the sols changed into wet gels, the wet gels were dried into xerogels by rotating evaporation at 80 °C. Then, the x% $Mg_2TiO_4$ doped CSZT xerogels and LNO xerogel were calcined 3 h at 1350 °C and 800 °C to form the x% $Mg_2TiO_4$ doped CSZT and LNO ceramic powdesr, respectively. Here, x% = 0, 2, 4, 6, and 8 in mol%, respectively. The deposition process of LNO buffer layer and x% $Mg_2TiO_4$-CSZT thin films were carried out on p-type Si substrates using a Radio Frequency Magnetron Sputtering system (RFMS, Sky Technology Development, JGP560D, Shenyang, China). The specific process parameters of x%-$Mg_2TiO_4$ CSZT films and LNO buffer layer are shown in Table 1. All the prepared thin films were conventional thermal annealed (CTA) in air at 700 °C for 180 min to obtain well-crystallized grains. A 0.3 mm diameter Au topped circular electrode was prepared on the CSZT layer by electroplating.

**Table 1.** The sputtering process parameters of x% $Mg_2TiO_4$-CSZT thin films and LNO buffer layer.

| Target | x% $Mg_2TiO_4$-CSZT | LNO |
|---|---|---|
| Substrate distance | 4 cm | 4 cm |
| Substrate rotation rate | 10–20 r/min | 10–20 r/min |
| Base vacuum | $4.0 \times 10^{-4}$ Pa | $4.0 \times 10^{-4}$ Pa |
| Sputtering temperature | 575 °C | 550 °C |
| Sputtering time | 600 min | 30 min |
| Sputtering power | 70 W | 40 W |
| Sputtering gas pressure | 2 Pa | 2 Pa |
| Sputtering atmosphere ratio | $Ar/O_2$ = 4:3 | $Ar/O_2$ = 4:1 |

The crystal phase of x% $Mg_2TiO_4$-CSZT thin films were measured using X ray-diffraction (DX-2700, Dandong, China) with Cu Kα radiation obtained under a Ni filter (Range: 2θ = 20°~70°, Step angle: 0.2°/step, Sampling time: 0.5 s/step, Tube voltage: 40 kV, Tube current: 30 mA). The thickness of the prepared thin films was investigated by field emission scanning electron microscope (Thermo Scientific, Helios G4 UC, Waltham, MA, USA) with an accelerating voltage of 15 kV. The capacitance–frequency curve (C-f curve)

from 10 kHz to 1 MHz and the capacitance-voltage curve (C-V curve) measured by using a multi-frequency Inductance-Capacitance-Resistance (LCR) meter (Agilent, HP4294A, Santa Clara, CA, USA), for C-V curve measurement, the thin films were measured with 100 kHz and a dielectric spectrum oscillation voltage of 500 mV at room temperature. The leakage current density of the prepared thin films was measured by using a Radiant Precision Workstation (Radiant, Precision Multiferroic II, Albuquerque, NM, USA) at room temperature. The temperature-related properties were carried on a heating probe stage (Linkam, HFS600E-PB4, Surrey, UK) with a temperature rising rate of 3 °C/min.

## 3. Results and Discussion

The XRD patterns of x% $Mg_2TiO_4$-CSZT thin films measured at room temperature are shown in Figure 1. The thin films were deposited on LNO/p-Si and annealed at 700 °C for 3 h. All the x% $Mg_2TiO_4$-CSZT thin films show the significant (l0l)-preferred orientation growth characteristic (according to PDF#35-0645). Clearly, the (l0l)-preferred orientated LNO buffer layer plays a key role here. Among them, the 0%, 2%, and 4%$Mg_2TiO_4$-CSZT thin film show the only perovskite phase. The 8% $Mg_2TiO_4$-CSZT thin film displays clear second phase diffraction peaks at ~43° and ~74° (marked with •). The two peaks are associated with the diffraction peaks of MgO (according to PDF# 87-0653). It suggests that $Mg_2TiO_4$-CSZT is limited solid solution and small amount of MgO separated out from the 8%$Mg_2TiO_4$ doped CSZT solid solution [25]. Furthermore, compared with pure CSZT thin film sample, the orientation of LNO buffer layers are weakened due to the growth of $Mg_2TiO_4$ doped CSZT thin film on them. As a result, the LNO (021) diffraction peaks could be observed in the $Mg_2TiO_4$ doped CSZT thin film XRD patterns. As a close observation, all the LNO (101) and (202) peaks (sited ~23°and ~47°) of those $Mg_2TiO_4$-CSZT thin film samples shift to left (see Figure 1). It is likely that the $Mg_2TiO_4$ doped CSZT interpenetrated the LNO layer at the interface, resulting in the orientation degree of LNO reducing, and more LNO diffraction peaks could be observed.

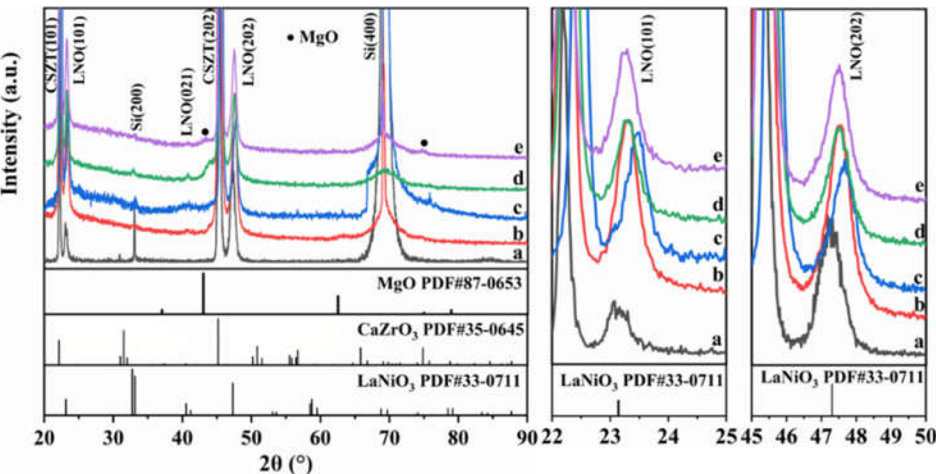


**Figure 1.** *X*-ray diffraction pattern of x% $Mg_2TiO_4$-CSZT thin films in the 2θ range of 20–90°. (**a**) x = 0; (**b**) x = 2; (**c**) x = 4; (**d**) x = 6; (**e**) x = 8.

Figure 2 shows cross-section morphology of the prepared thin films by SEM micrographs. All the thin films show dense, crack free, and uniform microstructure. The columnar crystalline grain of x% $Mg_2TiO_4$-CSZT grown on the LNO layer is clearly visible. Additionally, it could be noticed that the thicknesses of the thin films are different even though they were prepared in the same time. The thicknesses and growth rates of the thin films were listed in Table 2. The growth rate of the x% $Mg_2TiO_4$-CSZT thin films increases significantly with the increase in the $Mg_2TiO_4$ content when the content is more than 2%.

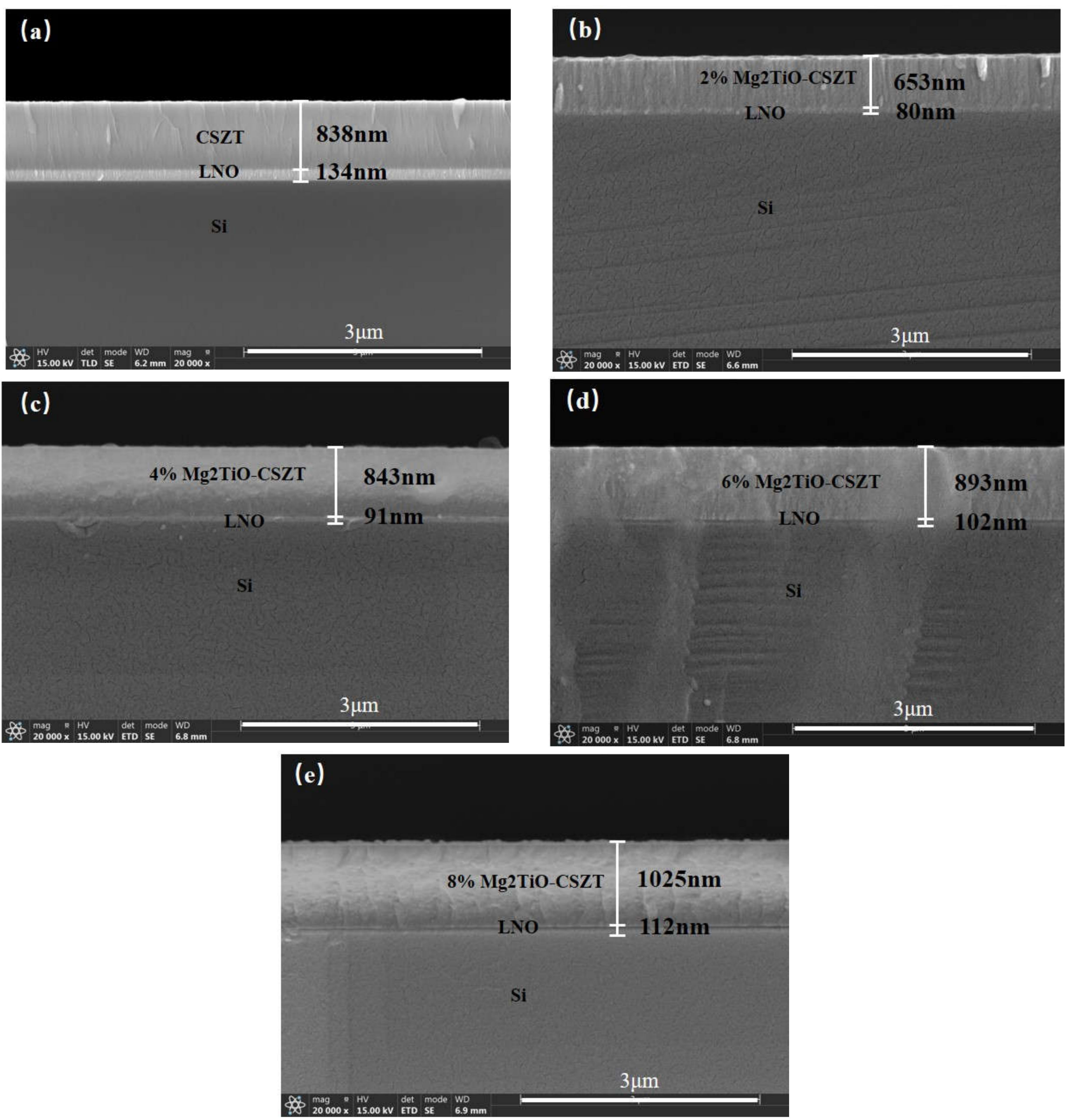


**Figure 2.** The cross-section scanning electron microscope (SEM) micrographs of the x% $Mg_2TiO_4$-CSZT/LNO thin films. (**a**) x = 0; (**b**) x = 2; (**c**) x = 4; (**d**) x = 6; (**e**) x = 8.

**Table 2.** The thickness and the growth rate of the x% $Mg_2TiO_4$-CSZT/LNO thin films.

| x (%) | 0 | 2 | 4 | 6 | 8 |
|---|---|---|---|---|---|
| Thickness of the x% $Mg_2TiO_4$-CSZT/LNO layer (nm) | 972 (±2) | 732 (±1) | 934 (±3) | 995 (±3) | 1137 (±2) |
| Growth rate of x% $Mg_2TiO_4$-CSZT films (nm/min) | 1.40 | 1.09 | 1.41 | 1.49 | 1.71 |

The dependence of DC voltage and frequency to dielectric permittivity and dielectric loss were measured at room temperature and shown in Figure 3. Both dielectric permittivity-frequency curve and the dielectric permittivity-DC voltage curve display the

frequency independent (see Figure 3a) and operating voltage independent (see Figure 3b) characteristics for all the prepared thin films. The results indicate that all the prepared thin films behave with a typical linear dielectric response, even the $Mg_2TiO_4$ doped CSZT thin films. Additionally, small amounts of $Mg_2TiO_4$ leads to a small increase in dielectric permittivity; the dielectric permittivity will reduce if the $Mg_2TiO_4$ content is higher than 4%.

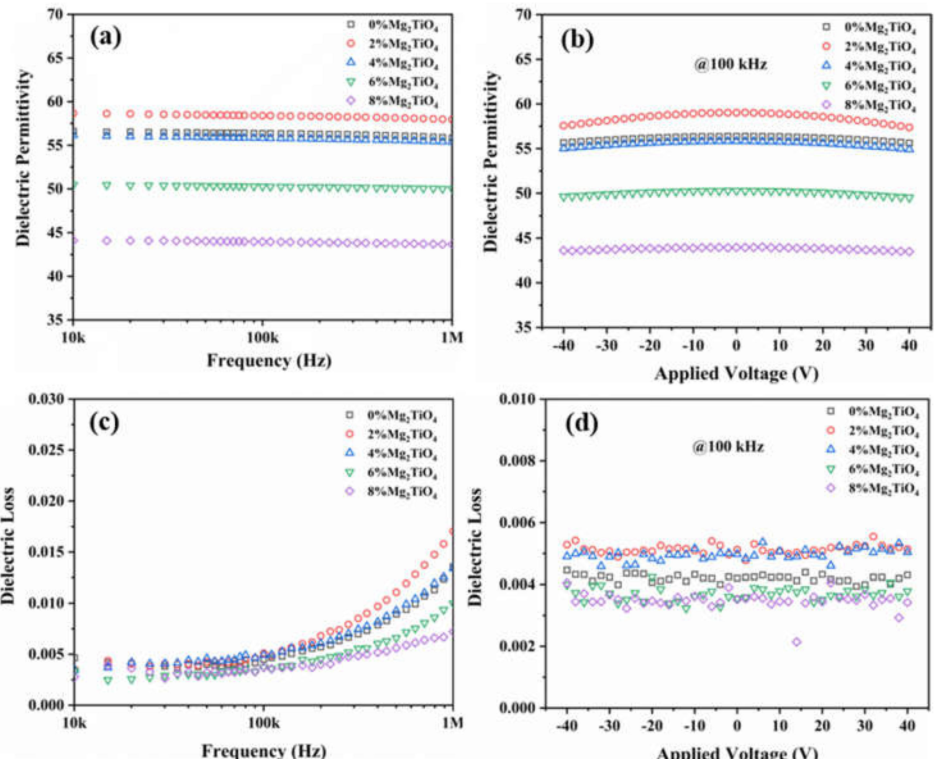


**Figure 3.** The dielectric properties of the prepared thin films at room temperature. (**a**,**b**) are the dielectric permittivity of x% $Mg_2TiO_4$-CSZT thin films as a function of frequency and DC voltage, respectively; (**c**,**d**) are the dielectric loss of x% $Mg_2TiO_4$-CSZT thin films as a function of frequency and DC voltage, respectively.

Figure 3c shows the dielectric loss-frequency curve of all the thin films. The dielectric loss of all the thin films is no mre than 0.0175 at 1 MHz. Figure 3d shows the DC field dependence of the dielectric loss (tanδ) of all the thin films. The measured signal is an AC signal with an amplitude of 0.5 V and a frequency of 100 kHz. The DC voltage ranges from −40 V to 40 V. The tanδ of all the thin films is no more than 0.006 in the measured range. The tanδ valus change rarely with the increase in voltage value, indicating the typical linear dielectric response feature which is consistent with the result of Figure 3b. For the thin film x = 6%, the dielectric permittivity $\varepsilon_r$ is around 50 at 1 MHz and tanδ is ~0.01 at 1 MHz which is lower than reported reference [10].

The dielectric response-temperature curve of x% $Mg_2TiO_4$-CSZT thin films is shown in Figure 4. The measured temperature ranges from −55 °C to 205 °C. Compared with the 0% $Mg_2TiO_4$–CSZT thin film, the dielectric permittivity of 6% $Mg_2TiO_4$-CSZT thin film shows the smallest temperature changing rate, the TCC value, ~−68 ppm/°C among all the prepared thin films. The TCC values of all the thin films ranging from −55 °C to 205 °C are around −135 ppm/°C, −98 ppm/°C, −78 ppm/°C, −68 ppm/°C, and −97 ppm/°C for x = 0, 2, 4, 6, and 8, respectively. The results reveal that moderate $Mg_2TiO_4$ are helpful to improve dielectric response-temperature characteristic. Meanwhile, the tanδ of the x% $Mg_2TiO_4$-CSZT thin films increase with the incerasing of temperature mildly below 100 °C, then the increase becomes significant and reaches 0.02 at 160 °C. For the thin films with x = 6 and 8, the tanδ values are still smaller than 0.01 at 120 °C. Compared with the other

linear dielectrics reported in the previous work (see Figure 5), 6% $Mg_2TiO_4$-CSZT thin film show ideal dielectric permittivity temperature stability, TCC value is second only to that of $SiO_2$. It is noticed that 6% $Mg_2TiO_4$-CSZT thin film keeps small temperature changing rate, TCC value (~−68) in a wide temperature range (−55 °C~205 °C).

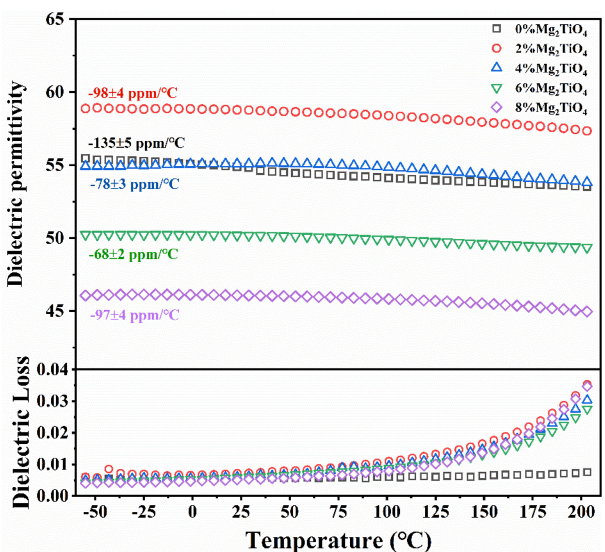


**Figure 4.** The dielectric response temperature characteristics of x% $Mg_2TiO_4$-CSZT thin films in the range of −55~205 °C.

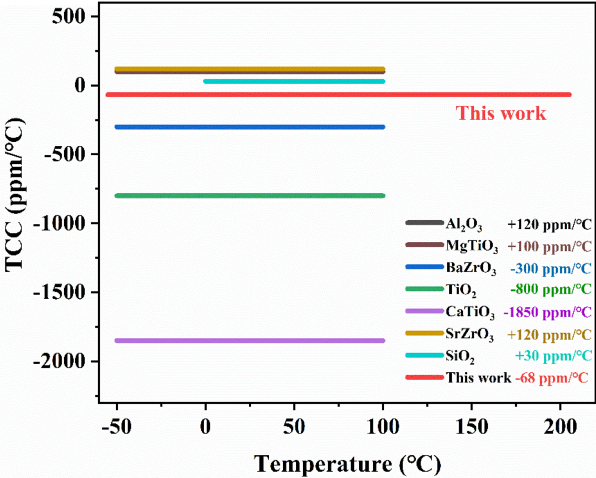


**Figure 5.** A TCC value comparison of this work and other reported linear dielectrics. Data are from references [26,27].

Figure 6 shows the leakage current density of the prepared x% $Mg_2TiO_4$-CSZT thin films at room temperature. The measured voltage ranges from −160 V to 160 V. At the voltage of 160 V, 8% $Mg_2TiO_4$-CSZT thin film has the lowest leakage current density ($1.61 \times 10^{-6}$ A/cm$^2$ at ±160 V), the leakage current density of 6% $Mg_2TiO_4$-CSZT thin film is $3.34 \times 10^{-6}$ A/cm$^2$ at ±160 V) which is lower than reported in reference [9] and [10]. The results indicate that the proper $Mg_2TiO_4$ introduction can decrease the leakage currents effectively.

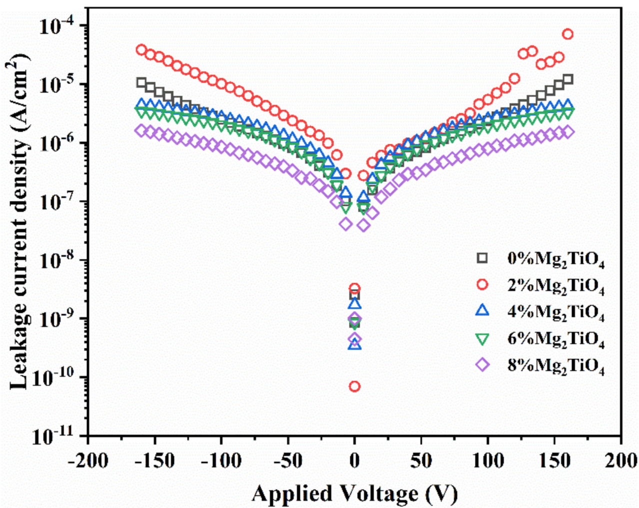


**Figure 6.** The leakage current density of x% $Mg_2TiO_4$-CSZT thin films as a function of the applied bias voltage at room temperature.

## 4. Conclusions

Investigations on the dielectric properties of x% $Mg_2TiO_4$-doped $Ca_{0.65}Sr_{0.35}Zr_{0.65}Ti_{0.35}O_3$ thin films showed that the addition of $Mg_2TiO_4$ can effectively reduce the dielectric loss and leakage current density of CSZT thin films. The prepared 6% $Mg_2TiO_4$-CSZT thin film exhibits a satisfying comprehensive performance of $\varepsilon_r$ ~50.00 at 1 MHz, tanδ ~0.01 at 1 MHz, TCC ~−68 ppm/°C from −55 °C to 205 °C, and about $3.34 \times 10^{-6}$ A/cm$^2$ at operating voltage of 160 V compared with the reported linear dielectrics given in reference [26,27], and thus could be a suitable capacitor material in the next generation portable electronic systems.

**Author Contributions:** Conceptualization, P.Y.; methodology, Y.L.; investigation, Y.L., B.H. and X.C.; data curation, Y.L.; writing—original draft preparation, Y.L.; writing—review and editing, P.Y.; project administration, P.Y.; funding acquisition, P.Y. All authors have read and agreed to the published version of the manuscript.

**Funding:** This research was funded by the National Natural Science Foundation of China under grant No. u1601208 and No. 51802204, China.

**Institutional Review Board Statement:** Not applicable.

**Informed Consent Statement:** Not applicable.

**Data Availability Statement:** Not applicable.

**Acknowledgments:** We appreciate Wang Hui from the Analytical and Testing Center of Sichuan University for her help with SEM characterization.

**Conflicts of Interest:** The authors declare no conflict of interest.

## References

1. Bhattacharya, S.K.; Tummala, R.R. Next generation integral passives: Materials, processes, and integration of resistors and capacitors on PWB substrates. *J. Mater. Sci. Mater. Electron.* **2000**, *11*, 253–268. [CrossRef]
2. Rahayu, R.; Kang, M.-G.; Do, Y.-H.; Hwang, J.-H.; Kang, C.-Y.; Yoon, S.-J. Electrical characteristics of $Ba_{0.6}Sr_{0.4}TiO_3$ Thin-film chip capacitors for embedded passive components. *IEEE Electron Device Lett.* **2013**, *34*, 99–101. [CrossRef]
3. Tuichai, W.; Danwittayakul, S.; Maensiri, S.; Thongbai, P. Investigation on Temperature stability performance of giant permittivity (In+Nb) in co–doped $TiO_2$ ceramic: A crucial aspect for practical electronic applications. *RSC Adv.* **2016**, *6*, 5582–5589. [CrossRef]
4. Chen, X.; Mo, T.; Huang, B.; Liu, Y.; Yu, P. Capacitance properties in $Ba_{0.3}Sr_{0.7}Zr_{0.18}Ti_{0.82}O_3$ Thin films on silicon substrate for thin film capacitor applications. *Crystals* **2020**, *10*, 318. [CrossRef]
5. Chen, X.; Zhang, Y.; Xie, B.; Huang, K.; Wang, Z.; Yu, P. Thickness-dependence of growth rate, dielectric response, and capacitance properties in $Ba_{0.67}Sr_{0.33}TiO_3/LaNiO_3$ hetero-structure thin films for film capacitor applications. *Thin Solid Film.* **2019**, *685*, 269–274. [CrossRef]

6. Groner, M.D.; Elam, J.W.; Fabreguette, F.H.; George, S.M. Electrical characterization of thin $Al_2O_3$ films grown by atomic layer deposition on silicon and various metal substrates. *Thin Solid Film.* **2002**, *413*, 186–197. [CrossRef]
7. Acquaviva, S.; Giorgi, M.L.D.; Elia, L.M.F.; Leggieri, G.; Luches, A.; Martino, M.; Zocco, A. Laser deposition of thin $SiO_2$ and ITO films. *Appl. Surf. Sci.* **2000**, *168*, 244–247. [CrossRef]
8. Chaneliere, C.; Autran, J.L.; Devine, R.A.B.; Balland, B. Tantalum pentoxide ($Ta_2O_5$) thin films for advanced dielectric applications. *Mater. Sci. Eng.* **1998**, *R22*, 269–322. [CrossRef]
9. Baek, E.; Yun, Y.S.; Kim, H.K.; Lee, S.H.; Lee, S.G.; Im, I.H.; Lee, Y.H. Effect of post-annealing on $(Ca_{0.7}Sr_{0.3})(Zr_{0.8}Ti_{0.2})O_3$ films on Pt and Cu substrates fabricated by aerosol deposition. *J. Nanosci. Nanotechnol.* **2015**, *15*, 8478–8483. [CrossRef]
10. Lee, S.H.; Kim, H.K.; Yun, Y.S.; Lee, S.G.; Lee, Y.H. Dielectric properties of $(Ca_{0.7}Sr_{0.3})(Zr_{0.8}Ti_{0.2})O_3$ thin films with different deposition temperatures. *J. Nanosci. Nanotechnol.* **2015**, *15*, 2330–2332. [CrossRef]
11. Huang, B.; Liu, Y.; Ji, H.; He, Q.; Chen, X.; Yu, P. Enhanced temperature stable dielectric response and high dielectric strength observed in $(CaZr)_{0.65}(SrTi)_{0.35}O_3$ thin film. *J. Alloy Compd.* **2021**, *876*, 160232. [CrossRef]
12. Zhai, J.; Yao, X.; Xu, Z.; Chen, H. Ferroelectric properties of $Pb_xSr_{1-x}TiO_3$ and its compositionally graded thin films grown on the highly oriented $LaNiO_3$ buffered Pt/Ti/$SiO_2$/Si substrates. *J. Appl. Phys.* **2006**, *100*, 034108. [CrossRef]
13. Cheng, Z.X.; Wang, X.L.; Kimura, H.; Ozawa, K.; Dou, S.X. La and Nb codoped $BiFeO_3$ multiferroic thin films on $LaNiO_3$/Si and $IrO_2$/Si substrates. *Appl. Phys. Lett.* **2008**, *92*, 092902. [CrossRef]
14. Tomczyk, M.; Mahajan, A.; Tkach, A.; Vilarinho, P.M. Interface-based reduced coercivity and leakage currents of $BiFeO_3$ thin films: A comparative study. *Mater. Des.* **2018**, *160*, 1322–1334. [CrossRef]
15. Gao, Y.; Yuan, M.; Sun, X.; Ouyang, J. In situ preparation of high quality $BaTiO_3$ dielectric films on Si at 350–500 °C. *J. Mater. Sci. Mater. Electron.* **2016**, *28*, 337–343. [CrossRef]
16. Meng, X.J.; Ma, Z.X.; Sun, J.L.; Bo, L.X.; Ye, H.J.; Guo, S.L.; Chu, J.H. Highly oriented $PbZr_{0.3}Ti_{0.7}O_3$ thin film on $LaNiO_3$-coated Si substrate derived from a chemical solution technique. *Thin Solid Film.* **2000**, *372*, 271–275. [CrossRef]
17. Sengupta, L.C.; Sengupta, S. Breakthrough advances in low loss, tunable dielectric materials. *Mater. Res. Innov.* **1999**, *2*, 278–282. [CrossRef]
18. Sengupta, L.; Warwick, M. Ceramic Ferroelectric Composite Material–BSTO–Magnesium Based Compound. U.S. Patent 5,635,434, 3 June 1997.
19. Chen, Y.; Dong, X.-L.; Liang, R.-H.; Li, J.-T.; Wang, Y.-L. Dielectric properties of $Ba_{0.6}Sr_{0.4}TiO_3$/$Mg_2SiO_4$/MgO composite ceramics. *J. Appl. Phys.* **2005**, *98*, 064107. [CrossRef]
20. Yan, L.; Chen, L.F.; Tan, C.Y.; Ong, C.K.; Anisur Rahman, M.; Osipowicz, T. $Ba_{0.1}Sr_{0.9}TiO_3$-$BaTi_4O_9$ composite thin films with improved microwave dielectric properties. *Eur. Phys. J. B Condens. Matter Complex Syst.* **2004**, *41*, 201–205. [CrossRef]
21. Jain, M.; Majumder, S.B.; Katiyar, R.S.; Agrawal, D.C.; Bhalla, A.S. Dielectric properties of sol–gel-derived MgO: $Ba_{0.5}Sr_{0.5}TiO_3$ thin-film composites. *Appl. Phys. Lett.* **2002**, *81*, 3212–3214. [CrossRef]
22. Jain, M.; Majumder, S.B.; Yuzyuk, Y.; Katiyar, R.S.; Bhalla, A.S.; Miranda, F.A.; Van Keuls, F.W. Dielectric properties and leakage current characteristics of sol-gel derived $(Ba_{0.5}Sr_{0.5})TiO_3$: $MgTiO_3$ thin film composites. *Ferroelectr. Lett.* **2003**, *30*, 99–107. [CrossRef]
23. Chou, X.; Zhai, J.; Yao, X. Dielectric tunable properties of low dielectric constant $Ba_{0.5}Sr_{0.5}TiO_3$–$Mg_2TiO_4$ microwave composite ceramics. *Appl. Phys. Lett.* **2007**, *91*, 122908. [CrossRef]
24. Gao, L.; Zhai, J.; Yao, X.; Xu, Z. $MgTiO_3$ and $Ba_{0.60}Sr_{0.40}Mg_{0.15}Ti_{0.85}O_3$ composite thin films with promising dielectric properties for tunable applications. *J. Am. Ceram. Soc.* **2008**, *91*, 3109–3112. [CrossRef]
25. Jia, Q.; Ji, H.; Li, X.; Liu, S.; Jin, Z. Sinterability and dielectric properties of $Ba_{0.55}Sr_{0.4}Ca_{0.05}TiO_3$–$CaTi_{Si}O_5$–$Mg_2TiO_4$ composite ceramics. *J. Alloy Compd.* **2011**, *509*, 10155–10160. [CrossRef]
26. Kell, R.C.; Greenham, A.C.; Olds, G.C.R. High-permittivity temperature-stable ceramic dielectrics with low microwave loss. *J. Am. Ceram. Soc.* **1973**, *56*, 352–354. [CrossRef]
27. Sato, S.; Sato, A.; Okamoto, E. An $SiO_2$-$Ta_2O_5$ thin film capacitor. *IEEE Trans. Parts Hybrids Packag.* **1973**, *9*, 161–166. [CrossRef]